

Nonreciprocal unidirectional and circular transmission in microcavity exciton polaritons

Hong-Ping Xu(徐红萍), Run-Run Yang(杨润润), Ji-Ming Gao(高吉明), and Zi-Fa Yu(鱼自发)

Citation: Chin. Phys. B, 2025, 34 (**11**): 114202. DOI: 10.1088/1674-1056/adee8c
http://cpb.iphy.ac.cn; http://iopscience.iop.org/cpb

What follows is a list of articles you may be interested in

Entropy evolution law of a general linear state for diffusion noise

Yingyu Zhang(张映玉) and Yixing Wang(王依兴)
Chin. Phys. B, 2025, 34 (**9**): 094206. DOI: 10.1088/1674-1056/add4f2

Quasi-two-dimensional isotropic laser cooling of atoms for quantum sensing

Xiao Zhang(张孝), Yi Song(宋屹), Yuan Sun(孙远), and Liang Liu(刘亮)
Chin. Phys. B, 2025, 34 (**8**): 084202. DOI: 10.1088/1674-1056/add4f7

Spectral photon-number distribution of parametric down-conversion and generation of heralded Fock states

Yan-Sheng Bao(包燕升), Bo-Chen Wang(王搏尘), Chang-Yong Tian(田昌勇), and Zheng-Yong Li(李政勇)
Chin. Phys. B, 2025, 34 (**7**): 074214. DOI: 10.1088/1674-1056/add904

Optical nonreciprocity in a piezo-optomechanical system

Yu-Ming Xiao(肖玉铭), Jun-Hao Liu(刘军浩), Qin Wu(吴琴), Ya-Fei Yu(於亚飞), Zhi-Ming Zhang(张智明)
Chin. Phys. B, 2020, 29 (**7**): 074204. DOI: 10.1088/1674-1056/ab8abf

Dynamically controlled optical nonreciprocity of a double-ladder system with spontaneously generated coherence in moving atomic optical lattice

Nuo Ba(巴诺), Xiang-Yao Wu(吴向尧), Dong-Fei Li(李东飞), Dan Wang(王丹), Jin-You Fei(费金有), Lei Wang(王磊)
Chin. Phys. B, 2017, 26 (**5**): 054207. DOI: 10.1088/1674-1056/26/5/054207

Nonreciprocal unidirectional and circular transmission in microcavity exciton polaritons

Hong-Ping Xu(徐红萍), Run-Run Yang(杨润润), Ji-Ming Gao(高吉明), and Zi-Fa Yu(鱼自发)†

College of Physics and Electronic Engineering, Northwest Normal University, Lanzhou 730070, China

(Received 19 March 2025; revised manuscript received 16 May 2025; accepted manuscript online 11 July 2025)

We investigate nonreciprocal transmission in microcavity exciton polaritons and obtain analytical conditions for achieving unidirectional and circular transmission. The phase difference between two effective optomechanical couplings can regulate the interference of different channels between two photon modes, and control the direction of nonreciprocity, resulting in unidirectional forward and backward transmissions. Perfect nonreciprocal unidirectional transmission with zero losses is realized, which depends on exciton–photon–phonon couplings. Moreover, clockwise and counterclockwise circular transmissions are implemented by appropriately adjusting the phase of photon mode couplings. Our results open up exciting possibilities for implementing nonreciprocal photonic devices.

Keywords: optical nonreciprocity, exciton polaritons, nonreciprocal photonic devices

PACS: 42.50.–p, 42.25.Bs, 71.36.+c, 42.79.Hp, 03.67.Lx

DOI: 10.1088/1674-1056/adee8c **CSTR:** 32038.14.CPB.adee8c

1. Introduction

As typical nonreciprocal transmission, unidirectional and circular transmission has attracted much attention, which can be used to implement isolators and circulators.[1,2] Traditional nonreciprocal transmission has been mainly realized by breaking Lorentz reciprocity in strong magnetic materials.[3,4] However, external magnetic fields and material losses result in nonreciprocal devices incovenient to integration and micromation with low insertion loss.[5,6] Cavity optomechanical systems have provided a magnetic-free and all-optical platform for realizing nonreciprocal transmission.[7–11] Especially, hybrid optomechanical systems formed by strong coupling between phonons, photons, and macroscopic quantum matters have become a popular means to achieve optical nonreciprocity,[12,13] where various of nonreciprocal phenomena have been revealed, such as nonreciprocal quantum-state conversion,[14] single-photon frequency converter,[15] and ground-state cooling.[16]

As a new and intriguing hybrid optomechanical system, microcavity exciton polaritons have attracted considerable interest since strong exciton–photon couplings are experimentally realized in GaAs/AlAs quantum-well microcavities.[17–19] Exciton polaritons inherit remarkable properties from their excitonic and photonic components, and demonstrate many outstanding features, such as strong nonlinear effects, low pump intensities, strong light–matter couplings, low dissipation rates, non-Hermitian, and nonequilibrium quantum characteristics. Hence, exciton polaritons have raised widespread interest in fundamental researches,[20–25] and provided an ideal platform for implementing advanced polaritonic devices.[26,27] Furthermore, strong exciton–photon coupling enables to effectively manipulate photon transmission, as well as the implementation of dissipative couplings between photon modes provides a possibility to regulate photon transmission along different directions. Such a photon transmission regulation in microcavity exciton polaritons provides an avenue for achieving nonreciprocal transmission, however, it is rarely explored so far.

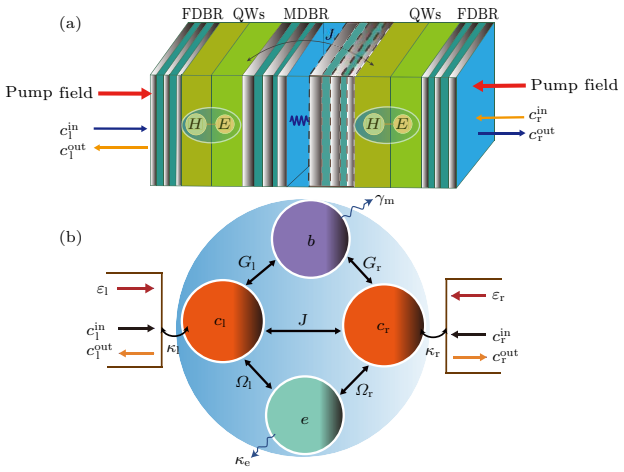


Fig. 1. (a) Schematic representation of a hybrid optomechanical system with microcavity exciton polaritons. (b) Schematic diagram of an equivalent four-mode hybrid optomechanical system.

In this paper, we construct a hybrid optomechanical system with a strong exciton–photon coupling to realize optical nonreciprocal transmission as shown in Fig. 1, and acquire analytical conditions for unidirectional and circular transmissions. We find that the phase difference between two effective optomechanical couplings can precisely manipulate the inter-

†Corresponding author. E-mail: Yuzifa@nwnu.edu.cn

© 2025 Chinese Physical Society and IOP Publishing Ltd. All rights, including for text and data mining, AI training, and similar technologies, are reserved.

ference of different channels between two photon modes, and control the direction of nonreciprocity, resulting in unidirectional forward and backward transmissions. In addition, we construct a hybrid three-mode system consisting of two photon modes and one exciton mode by eliminating optomechanical couplings, and design clockwise and counterclockwise circular transmissions. Our results can provide a promising means to achieve nonreciprocal photonic devices such as isolators and circulators.

2. Model

Motivated by experiments on microcavity exciton polaritons,[17–19] we consider a four-mode hybrid optomechanical system, which is constructed by a GaAs-spacer quantum-well microcavity consisting of two optical cavity modes (c_l and c_r, frequencies ω_l and ω_r), a phonon mode (b, frequency ω_m), and an exciton mode (e, frequency ω_e). Each optical cavity is constructed by a fixed distributed Bragg reflector (FDBR) a movable Bragg reflector (MDBR), and the MDBR acts as a phonon mode which couples two cavity modes. Excitons trapped in quantum wells (QWs) are placed at the antinode of each cavity field. In the quantum-well microcavity, strong exciton–photon coupling results in the emergence of new Bose quasiparticles, i.e., exciton polaritons, which can modulate photon transmission. The left (right) cavity is driven by an external strong pump field with an effective intensity ε_l (ε_r) and a frequency $\omega_\mathrm{dl}=\omega_\mathrm{dr}=\omega_\mathrm{d}$. Simultaneously, a weak quantum input field c_l^in (c_r^in) is incident on the left (right) cavity, while the corresponding output quantum field $c_\mathrm{l}^\mathrm{out}$ ($c_\mathrm{r}^\mathrm{out}$) is monitored at the left (right) cavity. In a rotating frame, the Hamiltonian is[28,29]

$$\begin{aligned} H \;=\; & \hbar\omega_\mathrm{m}\hat{b}^\dagger\hat{b}+\hbar\Delta_\mathrm{ld}\hat{c}_\mathrm{l}^\dagger\hat{c}_\mathrm{l}+\hbar\Delta_\mathrm{rd}\hat{c}_\mathrm{r}^\dagger\hat{c}_\mathrm{r}+\hbar\Delta_{e\mathrm{d}}\hat{e}^\dagger\hat{e} \\ & +J(\hat{c}_\mathrm{l}^\dagger\hat{c}_\mathrm{r}+\hat{c}_\mathrm{l}\hat{c}_\mathrm{r}^\dagger)+\sum_{i=\mathrm{l,r}}\hbar g_i\hat{c}_i^\dagger\hat{c}_i(\hat{b}^\dagger+\hat{b}) \\ & +\sum_{i=\mathrm{l,r}}\hbar\Omega_i(\hat{c}_i\hat{e}^\dagger+\hat{c}_i^\dagger\hat{e})+\sum_{i=\mathrm{l,r}}\mathrm{i}\hbar(\varepsilon_i\,\mathrm{e}^{\mathrm{i}\phi_i}\hat{c}_i^\dagger-\mathrm{H.c.}), \end{aligned} \tag{1}$$

where $\hat{c}_\mathrm{l}^\dagger$ ($\hat{c}_\mathrm{l}$), $\hat{c}_\mathrm{r}^\dagger$ ($\hat{c}_\mathrm{r}$), $\hat{b}^\dagger$ ($\hat{b}$), and $\hat{e}^\dagger$ ($\hat{e}$) correspond to the creation (annihilation) operators of left optical modes, right optical modes, phonon modes, and exciton modes, respectively. $\Delta_\mathrm{l,rd}=\omega_\mathrm{l,r}-\omega_\mathrm{d}$ and $\Delta_{e\mathrm{d}}=\omega_e-\omega_\mathrm{d}$ are the cavity–pump detuning and exciton–pump detuning, respectively. The fifth term describes a directly linear coupling between two optical modes with a coupling strength J. The sixth term represents a single photon optomechanical coupling between photons in the left (right) cavity and phonons with a coupling strength g_l (g_r). The seventh term refers to an exciton–photon coupling effect with a Rabi coupling strength Ω_i. The last term is a coherent driven cavity field, where ϕ_l and ϕ_r are the phases of pump fields coupled to the optical cavities c_l and c_r, respectively.

In experiments,[17–19,30–32] we construct a GaAs-spacer quantum-well microcavity which can be grown by molecular beam epitaxy on a 0.35-mm-thick GaAs substrate to realize nonreciprocal transmission, because the GaAs microcavity has many advantages, such as enhanced optical–mechanical couplings, perfect lattice matching of its compounds, and high fabrication compatibility with mature molecular beam epitaxy technology. However, conventional GaAs-based planar cavities suffer from weak exciton oscillator strength, small binding energy, as well as poor overlap between excitons and cavity modes due to the narrow quantum well layer, which results in the challenge of strong coupling and room-temperature operation. Interestingly, as typical wide bandgap materials, ZnO exhibits remarkable advantages for room-temperature exciton–polariton preparations due to larger exciton binding energy and oscillator strength.[33,34] Therefore, both GaAs/AlAs and ZnO materials can be used to construct an exciton–polariton system for realizing the nonreciprocal transmission. Moreover, two strong pump fields and two weak input quantum fields can be generated by picosecond light pulses delivering from a Ti:sapphire laser and split by a polarizing beam splitter. The linear coupling between different photon modes J is complex, which includes real and imaginary parts. The real photon–photon coupling refers to a directly coherent coupling and it can be induced in the presence of scattering off imperfections.[31] The imaginary photon–photon coupling refers to a dissipative coupling, which can be realized by the taper-scattering-induced dissipative backscattering.[32] According to experiments,[17–19] the performance parameters of microcavity exciton polaritons can be estimated as micropillar radius $r=1$ μm, GaAs substrate thickness $h=0.35$ mm, optical quality factor $Q_0=10^4$, cavity mode wavelength $\lambda_\mathrm{c}=870$ nm, QW thickness $L_\mathrm{f}=10$ nm, environment temperature $T=100$ K, pump power $P_\mathrm{pu}=300$ mW, pump spectral width $\Delta\lambda_\mathrm{pu}=0.8$ nm, $\kappa=1/5$ ps, $\Omega=0.48$ THZ $\sim\kappa$, $g=20$ MHz $\sim10^{-5}\kappa$, $\Delta_\mathrm{l,r}=210$ GHz $\sim0.1\kappa$, $\Delta_\mathrm{m}=8$ GHz $\sim0.01\kappa$, $\Delta_e=0.316$ THz $\sim\kappa$, $\gamma_\mathrm{m}=1/60$ ns $\sim10^{-3}\kappa$, and $\kappa_e=1/1.8$ ps $\sim2\kappa$.

Under strong pump fields, we assume that the operator can be written as a sum of its mean value and fluctuation, i.e., $\hat{o}=\langle\hat{o}\rangle+\delta\hat{o}$, where $o=\{c_\mathrm{l},c_\mathrm{r},b,e\}$. Inserting it into Eq. (1) and neglecting higher-order quantum fluctuation terms, we can acquire an effective linearized Hamiltonian

$$\begin{aligned} H_\mathrm{lin} \;=\; & \hbar\omega_\mathrm{m}\delta\hat{b}^\dagger\delta\hat{b}+\hbar\Delta'_\mathrm{ld}\delta\hat{c}_\mathrm{l}^\dagger\delta\hat{c}_\mathrm{l}+\hbar\Delta'_\mathrm{rd}\delta\hat{c}_\mathrm{r}^\dagger\delta\hat{c}_\mathrm{r} \\ & +\hbar\Delta_{e\mathrm{d}}\delta\hat{e}^\dagger\delta\hat{e}+\hbar J(\delta\hat{c}_\mathrm{r}\delta\hat{c}_\mathrm{l}{}^\dagger+\delta\hat{c}_\mathrm{l}\delta\hat{c}_\mathrm{r}{}^\dagger) \\ & +\sum_{i=\mathrm{l,r}}(\hbar\Omega_i\delta\hat{c}_i\delta\hat{e}^\dagger+\mathrm{H.c.})+\sum_{i=\mathrm{l,r}}(\hbar G_i\delta\hat{c}_i{}^\dagger\delta\hat{b}+\mathrm{H.c.}) \\ & +\sum_{i=\mathrm{l,r}}G_i\delta\hat{c}_i{}^\dagger\delta\hat{b}^\dagger, \end{aligned} \tag{2}$$

where $\Delta'_\mathrm{l,rd}=\Delta_\mathrm{l,rd}+g_\mathrm{l,r}(\langle\hat{b}\rangle+\langle\hat{b}^\dagger\rangle)$ is an effective cavity–pump detuning and $G_\mathrm{l,r}=g_\mathrm{l,r}\langle\hat{c}_\mathrm{l,r}\rangle$ represents an effective cou-

pling coefficient between optical modes and phonon modes. In order to analytically obtain the optical nonreciprocity in a four-mode hybrid optomechanical system, we introduce a unitary transformation $U = \mathrm{e}^{\mathrm{i}\omega_{\mathrm{d}}(\delta c_{\mathrm{l}}^{\dagger}\delta c_{\mathrm{l}}+\delta c_{\mathrm{r}}^{\dagger}\delta c_{\mathrm{r}}+\delta b^{\dagger}\delta b+\delta e^{\dagger}\delta e)t}$, and utilize rotating wave approximation in the high frequency region, then the linearized Hamiltonian Eq. (2) can be written as

$$\begin{aligned} H_{eff} &= 7\hbar\Delta_{\mathrm{m}}\delta\hat{b}^{\dagger}\delta\hat{b}+\hbar\Delta_{\mathrm{l}}\delta\hat{c}_{\mathrm{l}}^{\dagger}\delta\hat{c}_{\mathrm{l}}+\hbar\Delta_{\mathrm{r}}\delta\hat{c}_{\mathrm{r}}^{\dagger}\delta\hat{c}_{\mathrm{r}}+\hbar\Delta_{e}\delta\hat{e}^{\dagger}\delta\hat{e} \\ &\quad +\hbar J(\delta\hat{c}_{\mathrm{l}}\delta\hat{c}_{\mathrm{r}}{}^{\dagger}+\delta\hat{c}_{\mathrm{l}}{}^{\dagger}\delta\hat{c}_{\mathrm{r}})+\sum_{i=\mathrm{l,r}}(\hbar\Omega_i\delta\hat{c}_i\delta\hat{e}^{\dagger}+\mathrm{H.c.}) \\ &\quad +\sum_{i=\mathrm{l,r}}\hbar(G_i\delta\hat{c}_i{}^{\dagger}\delta\hat{b}+G_i^{*}\delta\hat{b}^{\dagger}\delta\hat{c}_i), \end{aligned} \tag{3}$$

where $\Delta_{\mathrm{l}} = \Delta'_{\mathrm{ld}} - \omega_{\mathrm{d}}$, $\Delta_{\mathrm{r}} = \Delta'_{\mathrm{rd}} - \omega_{\mathrm{d}}$, $\Delta_{\mathrm{m}} = \omega_{\mathrm{m}} - \omega_{\mathrm{d}}$, and $\Delta_e = \Delta_{ed} - \omega_{\mathrm{d}}$. Upon substituting Eq. (3) into the Heisenberg–Langevin equation $\partial_t\delta\hat{o} = (\mathrm{i}/\hbar)[H,\delta\hat{o}] + \hat{\mathcal{N}}$, where $\hat{\mathcal{N}}$ is the corresponding input vacuum noise operator, while using the commutation relation $[\hat{o},\hat{o}^{\dagger}] = 1$, the dynamical evolution of cavity modes, phonon modes, and exciton modes can be described by the following equations:

$$\begin{aligned} \delta\dot{c}_{\mathrm{l}} &= \left(-\mathrm{i}\Delta_{\mathrm{l}} - \frac{\kappa_{\mathrm{l}}}{2}\right)\delta c_{\mathrm{l}} - \mathrm{i}G_{\mathrm{l}}\delta b - \mathrm{i}J\delta c_{\mathrm{r}} - \mathrm{i}\Omega_{\mathrm{l}}\delta e + \sqrt{\kappa_{\mathrm{l}}}c_{\mathrm{l}}^{\mathrm{in}}, \\ \delta\dot{c}_{\mathrm{r}} &= \left(-\mathrm{i}\Delta_{\mathrm{r}} - \frac{\kappa_{\mathrm{r}}}{2}\right)\delta c_{\mathrm{r}} - \mathrm{i}G_{\mathrm{r}}\delta b - \mathrm{i}J\delta c_{\mathrm{l}} - \mathrm{i}\Omega_{\mathrm{r}}\delta e + \sqrt{\kappa_{\mathrm{r}}}c_{\mathrm{r}}^{\mathrm{in}}, \\ \delta\dot{b} &= \left(-\mathrm{i}\Delta_{\mathrm{m}} - \frac{\gamma_{\mathrm{m}}}{2}\right)\delta b - \mathrm{i}G_{\mathrm{l}}^{*}\delta c_{\mathrm{l}} - \mathrm{i}G_{\mathrm{r}}^{*}\delta c_{\mathrm{r}} + \sqrt{\gamma_{\mathrm{m}}}b^{\mathrm{in}}, \\ \delta\dot{e} &= \left(-\mathrm{i}\Delta_{e} - \frac{\kappa_{e}}{2}\right)\delta e - \mathrm{i}\Omega_{\mathrm{l}}\delta c_{\mathrm{l}} + \Omega_{\mathrm{r}}\delta c_{\mathrm{r}} + \sqrt{\kappa_{e}}e^{\mathrm{in}}, \end{aligned} \tag{4}$$

where $c_{\mathrm{l,r}}^{\mathrm{in}}$, b^{in}, and e^{in} are input field operators corresponding to cavity modes, phonon modes, and exciton modes with dissipation rates $\kappa_{\mathrm{l,r}}$, γ_{m}, and κ_e, respectively. For convenience, the linearized Langevin equation (4) can be written in the following form:

$$\frac{\mathrm{d}\boldsymbol{V}}{\mathrm{d}t} = \boldsymbol{M}\boldsymbol{V} + \boldsymbol{\Gamma}\boldsymbol{V}_{\mathrm{in}}, \tag{5}$$

where $\boldsymbol{V} = (\delta c_{\mathrm{l}}, \delta c_{\mathrm{r}}, \delta b, \delta e)^{\mathrm{T}}$ is a small quantum fluctuation vector, $\boldsymbol{V}_{\mathrm{in}} = (c_{\mathrm{l}}^{\mathrm{in}}, c_{\mathrm{r}}^{\mathrm{in}}, b^{\mathrm{in}}, e^{\mathrm{in}})^{\mathrm{T}}$ is the vector of input fields, $\boldsymbol{\Gamma}$ = diag$(\sqrt{\kappa_{\mathrm{l}}}, \sqrt{\kappa_{\mathrm{r}}}, \sqrt{\gamma_{\mathrm{m}}}, \sqrt{\kappa_e})$ is the dissipation matrix, and the matrix $\boldsymbol{M}$ is obtained as

$$\boldsymbol{M} = \begin{pmatrix} K_{\mathrm{l}} & -\mathrm{i}J & -\mathrm{i}G_{\mathrm{l}} & -\mathrm{i}\Omega_{\mathrm{l}} \\ -\mathrm{i}J & K_{\mathrm{r}} & -\mathrm{i}G_{\mathrm{r}} & -\mathrm{i}\Omega_{\mathrm{r}} \\ -\mathrm{i}G_{\mathrm{l}}^{*} & -\mathrm{i}G_{\mathrm{r}}^{*} & K_{\mathrm{m}} & 0 \\ -\mathrm{i}\Omega_{\mathrm{l}} & -\mathrm{i}\Omega_{\mathrm{r}} & 0 & K_e \end{pmatrix}, \tag{6}$$

with $K_{\mathrm{l,r},e} = -\kappa_{\mathrm{l,r,e}}/2 - \mathrm{i}\Delta_{\mathrm{l,r},e}$ and $K_{\mathrm{m}} = -\gamma_{\mathrm{m}}/2 - \mathrm{i}\Delta_{\mathrm{m}}$. To calculate the transmission spectrum of optical signals, we introduce a standard input–output relationship, i.e., $\boldsymbol{V}_{\mathrm{out}} = \boldsymbol{V}_{\mathrm{in}} - \boldsymbol{\Gamma}\boldsymbol{V}$ and a Fourier transform, i.e., $o(\omega) = \int_{-\infty}^{+\infty} o(t)\,\mathrm{e}^{\mathrm{i}\omega t}\,\mathrm{d}t/\sqrt{2\pi}$, then one can obtain

$$\boldsymbol{V}_{\mathrm{out}}(\omega) = [\boldsymbol{\Gamma}(\boldsymbol{M} - \mathrm{i}\omega)^{-1}\boldsymbol{\Gamma} - I]\boldsymbol{V}_{\mathrm{in}}(\omega) = \boldsymbol{T}(\omega)\boldsymbol{V}_{\mathrm{in}}(\omega), \tag{7}$$

where $\boldsymbol{V}_{\mathrm{out}} = (c_{\mathrm{l}}^{\mathrm{out}}, c_{\mathrm{r}}^{\mathrm{out}}, b^{\mathrm{out}}, e^{\mathrm{out}})^{\mathrm{T}}$. Equation (7) describes the optical signal transmission from modes i to j, where $i, j = c_{\mathrm{l}}, c_{\mathrm{r}}, b, e$ and the corresponding transmission efficiency is depicted by the matrix element T_{ij} of the transmission matrix $\boldsymbol{T}(\omega)$. The specific expression of matrix elements T_{ij} is obtained in Appendix A.

To investigate optical nonreciprocal unidirectional transmission, we define the forward (backward) transmission as the signal transmission from photon modes c_{l} (c_{r}) to c_{r} (c_{l}), and the corresponding forward (backward) transmission efficiency $T_{\rightleftarrows}(\omega)$ can be obtained as

$$\begin{aligned} T_{\rightleftarrows}(\omega) &= |\langle c_{\mathrm{r,l}}^{\mathrm{out}}/c_{\mathrm{l,r}}^{\mathrm{in}}\rangle|^2 = \kappa_{\mathrm{l}}\kappa_{\mathrm{r}}|T_{c_{\mathrm{l,r}}c_{\mathrm{r,l}}}|^2 \\ &= \kappa_{\mathrm{l}}\kappa_{\mathrm{r}}|(\mathrm{e}^{\pm\mathrm{i}\theta}G_{\mathrm{l}}G_{\mathrm{r}}/\widetilde{\omega}_{\mathrm{m}} \\ &\quad +\mathrm{i}J + \Omega_{\mathrm{l}}\Omega_{\mathrm{r}}/\widetilde{\omega}_e)\widetilde{\omega}_{\mathrm{m}}\widetilde{\omega}_e/F|^2. \end{aligned} \tag{8}$$

Equation (8) indicates that there are three possible channels for the signal transmission between photon modes c_{l} and c_{r}: one is direct channel ($c_{\mathrm{r}} \to c_{\mathrm{l}}$) measured by J, and the other two are indirect channels $c_{\mathrm{r}} \to e \to c_{\mathrm{l}}$ and $c_{\mathrm{r}} \to b \to c_{\mathrm{l}}$ measured by $\Omega_{\mathrm{l}}\Omega_{\mathrm{r}}/\widetilde{\omega}_e$ and $G_{\mathrm{l}}G_{\mathrm{r}}/\widetilde{\omega}_{\mathrm{m}}$, respectively. The phase difference θ between effective optomechanical couplings induces different direct and indirect channel interference effects for forward and backward transmissions, which results in unequal transmission efficiencies, i.e., $T_{\rightarrow}(\omega) \neq T_{\leftarrow}(\omega)$. This effect can be used to design undirectional transmission, and the direction can be controlled by phase differences.

Based on the difference of transmission directions, the nonreciprocity demonstrates as unidirectional forward transmission (i.e., $c_{\mathrm{l}} \to c_{\mathrm{r}}$) and unidirectional backward transmission (i.e., $c_{\mathrm{r}} \to c_{\mathrm{l}}$). Here, we focus on the unidirectional forward transmission, where the optical signal can be only transmitted from photon modes c_{l} to c_{r}, and the reversed transmission is blocked. To implement this nonreciprocity, the transmission from modes c_{r} to c_{l} should be destructive interference between direct and indirect channels, i.e., $T_{\leftarrow} = 0$, then, one can obtain the analytical condition for the nonreciprocal forward transmission

$$\theta = -\mathrm{Arg}[-\mathrm{i}J\widetilde{\omega}_{\mathrm{m}} - \widetilde{\omega}_{\mathrm{m}}\Omega_{\mathrm{l}}\Omega_{\mathrm{r}}/\widetilde{\omega}_e] + k\pi, \tag{9}$$

where k is integer. Moreover, to construct perfect nonreciprocity which is an ideal physical phenomenon, optical signals should be completely transmitted along the opposite direction ($c_{\mathrm{l}} \to c_{\mathrm{r}}$) without any loss, which means the signal from optical modes c_{l} should be completely transmitted to optical modes c_{r}, i.e., $T_{\rightarrow} = 1$, and there are no transmitted signals from modes c_{l} to modes b and e, i.e., $T_{c_{\mathrm{l}}b} = 0$ and $T_{c_{\mathrm{l}}e} = 0$. From $T_{c_{\mathrm{l}}b} = 0$ and $T_{c_{\mathrm{l}}e} = 0$, one can obtain

$$G_{\mathrm{r}}^2 = \frac{-\mathrm{e}^{2\mathrm{i}\theta}\widetilde{\omega}_{\mathrm{m}}(\widetilde{\omega}_{\mathrm{r}}\widetilde{\omega}_e + \Omega_{\mathrm{r}}^2)}{\widetilde{\omega}_e},$$

$$G_{\rm l}^2=\frac{|\widetilde{\omega}_{\rm m}({\rm i}J\widetilde{\omega}_e+\Omega_{\rm l}\Omega_{\rm r})|^2}{|\widetilde{\omega}_e|^2G_{\rm r}^2}. \tag{10}$$

Here, $G_{\rm l,r}$ refers to the amplitude of effective optomechanical coupling, and it should be reals, i.e., Im $G_{\rm r}=0$, thus, one has Im $[\widetilde{\omega}_{\rm m}(\widetilde{\omega}_{\rm r}\widetilde{\omega}_e+\Omega_{\rm r}^2)/\widetilde{\omega}_e]=0$ and $\theta\to k\pi+\pi/2$, i.e.,

$$\Omega_{\rm r}=\left[(4\Delta_e^2+\kappa_e^2)(\gamma_{\rm m}\Delta_{\rm r}+\Delta_{\rm m}\kappa_{\rm r})/(4\Delta_e\gamma_{\rm m}-4\Delta_{\rm m}\kappa_e)\right]^{1/2}. \tag{11}$$

and $\Delta_{\rm m}\ll\gamma_{\rm m}[J(4\Delta_e^2+\kappa_e^2)+2(\kappa_e-2\Delta_e)\Omega_{\rm l}\Omega_{\rm r}]/[2J(4\Delta_e^2+\kappa_e^2)-4(\kappa_e+2\Delta_e)\Omega_{\rm l}\Omega_{\rm r}]$.

From $T_{\rightarrow}=1$, ${\rm i}J(\widetilde{\omega}_e+2\Omega_{\rm l}\Omega_{\rm r})=(J^2\widetilde{\omega}_e+\Lambda)$, then, the critical optical mode coupling strength $J_{\rm c}$ reads

$$J_{\rm c}^2=[-\Lambda_1-(4|\widetilde{\omega}_e\Lambda|^2-\Lambda_1^2)^{\frac{1}{2}}]/(2|\widetilde{\omega}_e|^2), \tag{12}$$

where $\Lambda=|(\widetilde{\omega}_{\rm r}\widetilde{\omega}_e+\Omega_{\rm r}^2)(\widetilde{\omega}_{\rm l}\widetilde{\omega}_e+\Omega_{\rm l}^2)|$ and $\Delta_{e\omega}=\Delta_e-\omega$. In order to guarantee the optical coupling strength being real, $\Omega_{\rm l}$ should be restricted in a certain parameter region, i.e., $\Omega_{\rm l}<\Omega_{\rm l}^{\rm c}$.

Here, we focus on the dependence of perfect nonreciprocal transmission on the coupling between excitons and photons, and the enhancement and reduction effect of the transmission efficiency with respect to the coupling between excitons and photons become unimportant. Actually, the condition for perfect nonreciprocal transmission closely depends on the coupling between excitons and photons. Equations (9)–(12) describe analytical conditions for perfect nonreciprocal transmission, which is clearly displayed in Fig. 2. Under the condition of nonreciprocity [Eq. (9)], the transmission from photon modes $c_{\rm r}$ to $c_{\rm l}$ is completely prohibited, i.e., $T_{\leftarrow}=0$, which means a nonreciprocal unidirectional forward transmission occurs. When $\Omega_{\rm l}<\Omega_{\rm l}^{\rm c}$ and $J=J_{\rm c}$ [Eq. (12)], i.e., the condition for perfect nonreciprocity is satisfied, the photon can be completely transmitted from photon modes $c_{\rm l}$ to $c_{\rm r}$ without any losses (where $T_{\rightarrow}=1$), which means a perfect nonreciprocal forward transmission occurs [Fig. 2(a)]. However, when $\Omega_{\rm l}>\Omega_{\rm l}^{\rm c}$, no matter the optical coupling strength J is, $T_{\rightarrow}$ is always less than one [Fig. 2(b)], i.e., the forward transmission is always accompanied with losses. This transmission is called as an unperfect nonreciprocal transmission. In fact, energy losses of the system are inevitable in practical applications, however, our system is always driven by the strong pump field which can balance the intrinsic energy loss. Thus, the perfect nonreciprocal transmission with zero losses is a universal phenomenon and an ideal condition is not required.

The nonreciprocity can also be described by the nonreciprocal contrast $\chi=(T_{\rightarrow}-T_{\leftarrow})/(T_{\rightarrow}+T_{\leftarrow})$. When $\chi=100\%$, the nonreciprocal unidirectional forward transmission appears as shown in Figs. 2(c) and 2(d). The perfect nonreciprocity can also be characterized by the insertion loss, and the forward insertion loss is defined as IL $=-10\lg[\sqrt{T_{\rightarrow}}]$. The zero insertion loss indicates the emergence of a perfect nonreciprocity, where $J=J_{\rm c}$ as shown in Fig. 2(c), and when the insertion loss IL >0, the nonreciprocal transmission is unperfect. When $\Omega_{\rm l}<\Omega_{\rm l}^{\rm c}$, the critical optical mode coupling strength $J_{\rm c}$ for perfect nonreciprocity is slowly enhanced as $\Omega_{\rm l}$ increases.

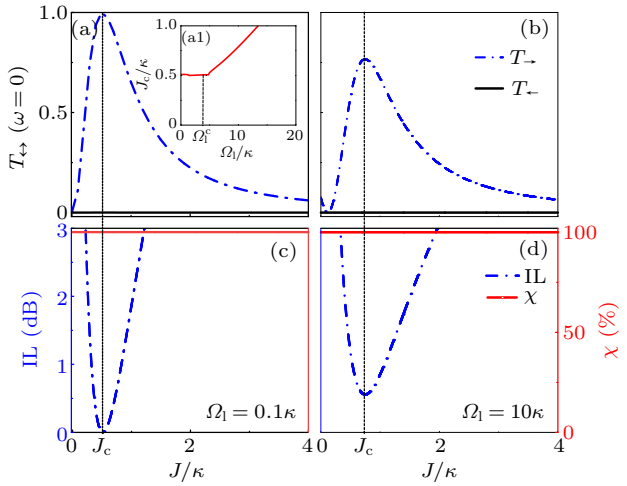


Fig. 2. Nonreciprocal unidirectional transmission. Forward (backward) transmission efficiency $T_{\rightarrow}$ ($T_{\leftarrow}$) versus J for a perfect nonreciprocal transmission (a), an unperfect one (b), and the corresponding insertion loss IL and nonreciprocal contrast χ (c)–(d). The inset (a1) depicts the critical optical mode coupling strength $J_{\rm c}$ for perfect nonreciprocity versus $\Omega_{\rm l}$. Other parameters are $\omega=0$, $\Delta_{\rm l}=\Delta_{\rm r}=0.01\kappa$, $\Delta_{\rm m}=10^{-5}\kappa$, $\Delta_e=10\kappa$, $\kappa_{\rm l}=\kappa_{\rm r}=\kappa$, $\gamma_{\rm m}=10^{-3}\kappa$, and $\kappa_e=0.1\kappa$.

On the other hand, the nonreciprocal transmission direction can also be controlled by the phase difference between effective optomechanical couplings. Here, the phase difference θ depends not only on the coupling coefficients, detuning, and dissipation rates but also on the pump field intensity $\varepsilon_{\rm l,r}$ and phase $\phi_{\rm l,r}$. When other parameters are fixed, θ can be directly controlled by adjusting $\varepsilon_{\rm l,r}$ and $\phi_{\rm l,r}$. Conversely, if other parameters vary, $\varepsilon_{\rm l,r}$ and $\phi_{\rm l,r}$ can be precisely tuned to maintain a constant θ. Such adjustments can be easily realized in experiments.[18,35] As depicted in Fig. 3, under the condition for perfect nonreciprocity, if the phase difference $\theta\approx-\pi/2$ which satisfies the condition for nonreciprocal forward transmission [Eq. (9)], $T_{c_{\rm r}\to c_{\rm l}}=0$ and $T_{c_{\rm l}\to c_{\rm r}}=1$. Namely, perfect forward nonreciprocity is discovered. One the contrary, $\theta\approx\pi/2$, $T_{c_{\rm r}\to c_{\rm l}}=1$, and $T_{c_{\rm l}\to c_{\rm r}}=0$, which indicates that perfect backward nonreciprocity arises.

Moreover, perfect nonreciprocity can be accurately manipulated by exciton–photon Rabi couplings, which is clearly shown in Fig. 4. When the condition of perfect nonreciprocity is satisfied, i.e., $\Omega_{\rm l}<\Omega_{\rm l}^{\rm c}$ and $J=J_{\rm c}$ [see Eq. (12)], an perfect nonreciprocal forward transmission with zero losses is observed, i.e., $T_{\rightarrow}=1$, $T_{\leftarrow}=0$, IL $=0$, and $\chi=100\%$ [see Figs. 4(a) and 4(b)]. When $\Omega_{\rm l}>\Omega_{\rm l}^{\rm c}$, even though $J=J_{\rm c}$, there are still losses in the nonreciprocal forward transmission, i.e.,

$T_{\rightarrow} < 1$, IL > 0. These results are in good agreement with analytical conditions for perfect nonreciprocity. Figures 4(c) and 4(d) indicate that the region of $\Omega_{\rm l}$ for perfect nonreciprocity is enlarged by increasing the effective exciton–pump detuning Δ_e.

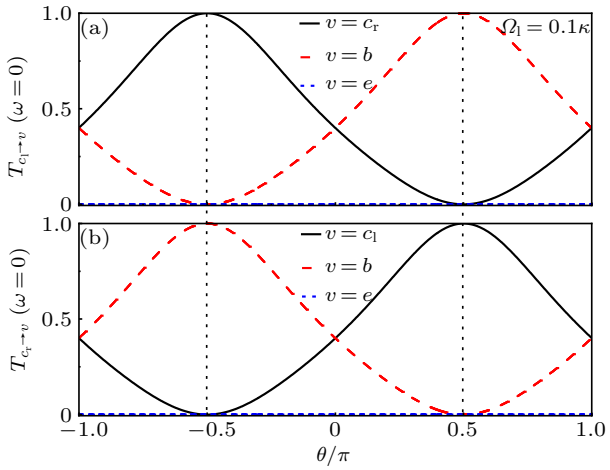


Fig. 3. Controlling nonreciprocal unidirectional transmission direction. (a) Forward [(b) backward] transmission efficiency $T_{c_{\rm l}\rightarrow v}$ ($T_{c_{\rm r}\rightarrow v}$) versus θ. Other parameters are the same as those in Fig. 2.

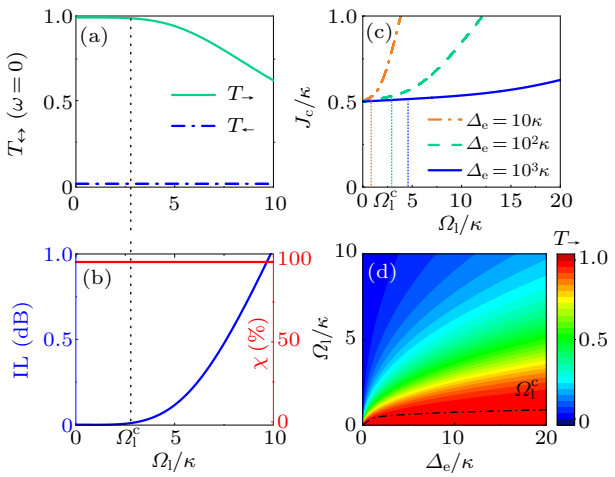


Fig. 4. Controlling perfect nonreciprocal unidirectional transmission. (a)–(c) Forward (backward) transmission efficiency $T_{\rightarrow}$ ($T_{\leftarrow}$), insertion loss IL and nonreciprocal contrast χ, and critical optical mode coupling strength $J_{\rm c}$ for perfect nonreciprocity versus $\Omega_{\rm l}$. (d) Forward transmission efficiency $T_{\rightarrow}$ in Δ_e–$\Omega_{\rm l}$ plane. Other parameters are the same as those in Fig. 2.

3. Nonreciprocal circular transmission

To obtain analytical conditions for circular transmission and realize perfect circular transmission, we construct a hybrid three-mode system consisting of an exciton mode and two photon modes by eliminating the single photon optomechanical coupling between photon and phonon modes, i.e., $g_{\rm l} = g_{\rm r} \equiv 0$. Meanwhile, weak quantum input field $e^{\rm in}$ and the corresponding output field $e^{\rm out}$ are added at the side of exciton modes as shown in Fig. 5(a). To generate clockwise and counterclockwise nonreciprocal circular transmissions as well as control the direction of circular transmission, we introduce a dissipative coupling between two optical modes, i.e., $J = Je^{{\rm i}\varphi}$. Then, the switching between clockwise and counterclockwise transmissions can be regulated by the phase φ (see the transmission coefficients for circular transmission in Appendix A).

For clockwise circular transmission, optical signals are transmitted along a clockwise direction (i.e., $c_{\rm l} \rightarrow c_{\rm r} \rightarrow e \rightarrow c_{\rm l}$) and the counterclockwise transmission is completely suppressed, i.e., $|T_{ec_{\rm l}}|^2 = |T_{c_{\rm l}c_{\rm r}}|^2 = |T_{c_{\rm r}e}|^2 = 1$ and $T_{c_{\rm l}e} = T_{ec_{\rm r}} = T_{c_{\rm r}c_{\rm l}} = 0$. From $T_{c_{\rm r}c_{\rm l}} = 0$, one can obtain

$$\varphi = {\rm Arg}[{\rm i}\Omega_{\rm l}\Omega_{\rm r}/\widetilde{\omega}_e] + k\pi, \quad J = |\Omega_{\rm r}\Omega_{\rm l}/\widetilde{\omega}_e|, \tag{13}$$

where k is integers. Moreover, upon inserting Eq. (13) into $T_{c_{\rm l}e} = 0$ and $T_{ec_{\rm r}} = 0$, one can obtain

$$\Omega_{\rm r,l} = \sqrt{\kappa_{\rm l,r}\kappa_e/4 + \kappa_{\rm l,r}\Delta_e^2/\kappa_e}. \tag{14}$$

Here, $\Omega_{\rm r,l}$ should be reals, thus, one has $\Delta_{\rm l,r} = -\Delta_e\kappa_{\rm l,r}/\kappa_e$.

Equations (13) and (14) describe analytical conditions for circular transmission along a clockwise direction. As shown in Figs. 5(c)–5(e), when the condition of Eq. (13) is satisfied and $\Omega_{\rm r}$ meets with Eq. (14), $T_{c_{\rm r}c_{\rm l}} = T_{c_{\rm l}e} = 0$ and $|T_{c_{\rm r}e}|^2 = 1$, while when $\Omega_{\rm l}$ is adjusted to satisfy Eq. (14), $|T_{c_{\rm l}c_{\rm r}}|^2 = |T_{ec_{\rm l}}|^2 = 1$ and $T_{ec_{\rm r}} = 0$, which indicates that perfect clockwise circular transmission occurs. Moreover, when the condition of Eq. (14) is satisfied, the circular transmission along clockwise and counterclockwise directions can be manipulated by the phase φ. As shown in Fig. 5(b), where we define $T_{\circlearrowright} = (|T_{c_{\rm l}e}|^2 + |T_{ec_{\rm r}}|^2 + |T_{c_{\rm r}c_{\rm l}}|^2)/3$ and $T_{\circlearrowleft} = (|T_{ec_{\rm l}}|^2 + |T_{c_{\rm l}c_{\rm r}}|^2 + |T_{c_{\rm r}e}|^2)/3$, clockwise circular transmission appears for $\varphi \approx \pi/2$ and counterclockwise transmission arises for $\varphi \approx -\pi/2$.

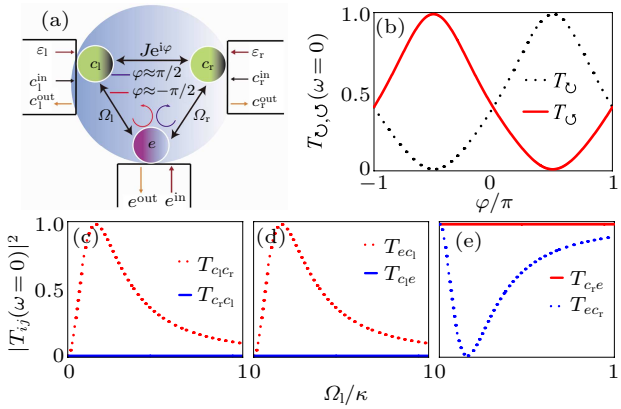


Fig. 5. Controlling circular transmission, (a) schematic diagram for circular transmission, (b) clockwise and counterclockwise transmission efficiency $T_{\circlearrowright,\circlearrowleft}$ versus phase φ of photon mode couplings, (c)–(e) the transmission efficiency T_{ij} between different modes versus $\Omega_{\rm l}$. Other parameters are $\Delta_e = 10^{-3}\kappa$, $\kappa_{\rm l} = \kappa_{\rm r} = \kappa$, and $\kappa_e = 0.1\kappa$.

4. Conclusion

In summary, we have demonstrated optical nonreciprocity in a microcavity exciton–polariton system and obtained analytical conditions for achieving nonreciprocal transmission

and circular transmission. We have proven that unidirectional nonreciprocity is achieved by adjusting the phase difference between two effective optomechanical couplings to induce the breaking of time reversal symmetry and the direction of nonreciprocal unidirectional transmission can be precisely regulated. We have also realized perfect unidirectional transmission with zero losses by adjusting the coupling among excitons, photons, and phonons. Moreover, we have presented clockwise and counterclockwise circular transmissions in a three-mode system consisting of an exciton and two photon modes by adjusting the phase of photon mode couplings, which can be used to design an optomechanical circulator. Although our proposed nonreciprocal transmission can be realized in experiments under current experimental conditions, there are some challenges in several critical steps,[36] such as resonant mode matching, quality factor limitations, and system integration complexities. We believe, however, that such devices for nonreciprocal transmission are achievable with continued advances in optics and microfabrication technology. Our results provide a promising avenue for implementing nonreciprocal photonic devices, which may have potential applications in developing macroscopic chiral quantum information and on-chip quantum communications.[37]

Appendix A: Specific representations of transmission efficiency matrix elements

From Eq. (6), we can acquire

$$\begin{aligned}\boldsymbol{T}(\omega) &= \Gamma(M-\mathrm{i}\omega)^{-1}\Gamma - I \\ &= \begin{pmatrix} T_{c_\mathrm{l}c_\mathrm{l}} & T_{c_\mathrm{l}c_\mathrm{r}} & T_{c_\mathrm{l}b} & T_{c_\mathrm{l}e} \\ T_{c_\mathrm{r}c_\mathrm{l}} & T_{c_\mathrm{r}c_\mathrm{r}} & T_{c_\mathrm{r}b} & T_{c_\mathrm{r}e} \\ T_{bc_\mathrm{l}} & T_{bc_\mathrm{r}} & T_{bb} & T_{be} \\ T_{ec_\mathrm{l}} & T_{ec_\mathrm{r}} & T_{eb} & T_{ee} \end{pmatrix},\end{aligned} \tag{A1}$$

where the matrix elements T_{ij} $(i,j = c_\mathrm{l}, c_\mathrm{r}, b, e)$ correspond to the transmission coefficients of signals from modes i to j. Here, we set $G_{\mathrm{l,r}}\mathrm{e}^{\mathrm{i}\theta_{\mathrm{l,r}}}$, i.e., the effective optomechanical coupling is expressed as a function of its amplitude and phase. Then, the specific form of the element T_{ij} is obtained as

$$\begin{aligned}
T_{c_\mathrm{l}c_\mathrm{l}} &= \kappa_\mathrm{l}[G_\mathrm{r}^2\widetilde{\omega}_e + \widetilde{\omega}_\mathrm{m}Z_1]/F - 1, \\
T_{c_\mathrm{r}c_\mathrm{l}} &= \sqrt{\kappa_\mathrm{l}\kappa_\mathrm{r}}[\mathrm{e}^{-\mathrm{i}\theta}G_\mathrm{l}G_\mathrm{r}\widetilde{\omega}_e + \widetilde{\omega}_\mathrm{m}Z_2]/F, \\
T_{bc_\mathrm{l}} &= \sqrt{\kappa_\mathrm{l}\gamma_\mathrm{m}}\mathrm{e}^{\mathrm{i}\theta_\mathrm{r}}[-\mathrm{i}G_\mathrm{r}Z_2 + \mathrm{i}\,\mathrm{e}^{-\mathrm{i}\theta}G_\mathrm{l}Z_1]/F, \\
T_{ec_\mathrm{l}} &= \sqrt{\kappa_\mathrm{l}\kappa_e}[\mathrm{i}\Omega_\mathrm{l} + J\widetilde{\omega}_\mathrm{m}\Omega_\mathrm{r} - \mathrm{i}\,\mathrm{e}^{-\mathrm{i}\theta}G_\mathrm{l}G_\mathrm{r}\Omega_\mathrm{r}]/F, \\
T_{c_\mathrm{l}c_\mathrm{r}} &= \sqrt{\kappa_\mathrm{l}\kappa_\mathrm{r}}[\mathrm{e}^{\mathrm{i}\theta}G_\mathrm{l}G_\mathrm{r}\widetilde{\omega}_e + \widetilde{\omega}_\mathrm{m}Z_2]/F, \\
T_{c_\mathrm{r}c_\mathrm{r}} &= \kappa_\mathrm{r}[G_\mathrm{l}^2\widetilde{\omega}_e + \widetilde{\omega}_\mathrm{m}Z_4]/F - 1, \\
T_{bc_\mathrm{r}} &= \sqrt{\kappa_\mathrm{r}\gamma_\mathrm{m}}\mathrm{e}^{\mathrm{i}\theta_\mathrm{l}}[-\mathrm{i}G_\mathrm{l}Z_2 + \mathrm{i}\,\mathrm{e}^{\mathrm{i}\theta}G_\mathrm{r}Z_4]/F, \\
T_{ec_\mathrm{r}} &= \sqrt{\kappa_\mathrm{r}\kappa_e}[\mathrm{i}Z_5\Omega_\mathrm{r} - \mathrm{i}\,\mathrm{e}^{\mathrm{i}\theta}G_\mathrm{l}G_\mathrm{r}\Omega_\mathrm{l} + J\widetilde{\omega}_\mathrm{m}\Omega_\mathrm{l}]/F, \\
T_{c_\mathrm{l}b} &= \sqrt{\kappa_\mathrm{l}\gamma_\mathrm{m}}\mathrm{e}^{-\mathrm{i}\theta_\mathrm{r}}[-\mathrm{i}G_\mathrm{r}Z_2 + \mathrm{i}\,\mathrm{e}^{\mathrm{i}\theta}G_\mathrm{l}Z_1]/F,
\end{aligned} \tag{A2}$$

$$\begin{aligned}
T_{c_\mathrm{r}b} &= \sqrt{\gamma_\mathrm{m}\kappa_\mathrm{r}}\mathrm{i}\,\mathrm{e}^{-\mathrm{i}\theta_\mathrm{l}}[-\mathrm{i}G_\mathrm{l}Z_2 + \mathrm{i}\,\mathrm{e}^{-\mathrm{i}\theta}G_\mathrm{r}Z_4]/F, \\
T_{bb} &= \gamma_\mathrm{m}[J^2\widetilde{\omega}_e + \widetilde{\omega}_\mathrm{r}\Omega_\mathrm{l}^2 - 2\mathrm{i}J\Omega_\mathrm{l}\Omega_\mathrm{r} + \widetilde{\omega}_\mathrm{l}Z_1]/F - 1, \\
T_{eb} &= \sqrt{\gamma_\mathrm{m}\kappa_e}\,\mathrm{e}^{-\mathrm{i}\theta_\mathrm{r}}[G_\mathrm{r}Z_6 + \mathrm{e}^{\mathrm{i}\theta}G_\mathrm{l}Z_7]/F,
\end{aligned} \tag{A4}$$

$$\begin{aligned}
T_{c_\mathrm{l}e} &= \sqrt{\kappa_\mathrm{l}\kappa_e}[\mathrm{i}Z_3\Omega_\mathrm{l} - \mathrm{i}\,\mathrm{e}^{-\mathrm{i}\theta}G_\mathrm{l}G_\mathrm{r}\Omega r + J\widetilde{\omega}_\mathrm{m}\Omega_\mathrm{r}]/F, \\
T_{c_\mathrm{r}e} &= \sqrt{\kappa_e\kappa_\mathrm{r}}[\mathrm{i}Z_5\Omega_\mathrm{r} + J\widetilde{\omega}_\mathrm{m}\Omega_\mathrm{l} - \mathrm{i}\,\mathrm{e}^{-\mathrm{i}\theta}G_\mathrm{l}G_\mathrm{r}\Omega_\mathrm{l}]/F, \\
T_{be} &= \sqrt{\kappa_e\gamma_\mathrm{m}}\,\mathrm{e}^{\mathrm{i}\theta_\mathrm{r}}[G_\mathrm{r}Z_6 + \mathrm{e}^{-\mathrm{i}\theta}G_\mathrm{l}Z_7]/F, \\
T_{ee} &= \kappa_e(G_\mathrm{r}^2\widetilde{\omega}_\mathrm{l} + G_\mathrm{l}^2\widetilde{\omega}_\mathrm{r} + \widetilde{\omega}_\mathrm{m}Z_8 - 2\mathrm{i}\cos\theta G_\mathrm{l}G_\mathrm{r}J)/F - 1,
\end{aligned} \tag{A5}$$

where $\widetilde{\omega}_\mathrm{l} = \kappa_\mathrm{l}/2 + \mathrm{i}(\Delta_\mathrm{l} - \omega)$, $\widetilde{\omega}_\mathrm{r} = \kappa_\mathrm{r}/2 + \mathrm{i}(\Delta_\mathrm{r} - \omega)$, $\widetilde{\omega}_\mathrm{m} = \gamma_\mathrm{m}/2 + \mathrm{i}(\Delta_\mathrm{m} - \omega)$, $\widetilde{\omega}_e = \kappa_e/2 + \mathrm{i}(\Delta_e - \omega)$, $\theta = \theta_\mathrm{r} - \theta_\mathrm{l}$, $Z_{1,4} = \widetilde{\omega}_{\mathrm{r,l}}\widetilde{\omega}_e + \Omega_{\mathrm{r,l}}^2$, $Z_2 = \mathrm{i}J\widetilde{\omega}_e + \Omega_\mathrm{l}\Omega_\mathrm{r}$, $Z_{3,5} = G_{\mathrm{r,l}}^2 + \widetilde{\omega}_{\mathrm{r,l}}\widetilde{\omega}_\mathrm{m}$, $Z_{6,7} = \widetilde{\omega}_{\mathrm{l,r}}\Omega_{\mathrm{r,l}} - \mathrm{i}J\Omega_{\mathrm{l,r}}$, $Z_8 = J^2 + \widetilde{\omega}_\mathrm{l}\widetilde{\omega}_\mathrm{r}$, and $F = G_\mathrm{r}^2(\widetilde{\omega}_\mathrm{l}\widetilde{\omega}_e + \Omega_\mathrm{l}^2) + G_\mathrm{l}^2(\widetilde{\omega}_\mathrm{r}\widetilde{\omega}_e + \Omega_\mathrm{r}^2) + \widetilde{\omega}_\mathrm{m}[J^2\widetilde{\omega}_e + \widetilde{\omega}_\mathrm{r}\Omega_\mathrm{l}^2 - 2\mathrm{i}J\Omega_\mathrm{l}\Omega_\mathrm{r} + \widetilde{\omega}_\mathrm{l}(\widetilde{\omega}_\mathrm{r}\widetilde{\omega}_e + \Omega_\mathrm{r}^2)] + 2G_\mathrm{l}G_\mathrm{r}(-\mathrm{i}J\widetilde{\omega}_e - \Omega_\mathrm{l}\Omega_\mathrm{r})\cos\theta$.

For nonreciprocal circular transmission, transmission efficiency matrix elements are obtained as

$$\begin{aligned}
T_{c_\mathrm{l}c_\mathrm{l}} &= \kappa_\mathrm{l}(-\widetilde{\omega}_\mathrm{r}\widetilde{\omega}_e - \Omega_\mathrm{r}^2)/f - 1, \\
T_{c_\mathrm{l}c_\mathrm{r}} &= \sqrt{\kappa_\mathrm{l}\kappa_\mathrm{r}}(\mathrm{i}\,\mathrm{e}^{-\mathrm{i}\varphi}J\widetilde{\omega}_e + \Omega_\mathrm{l}\Omega_\mathrm{r})/f, \\
T_{c_\mathrm{l}e} &= \sqrt{\kappa_\mathrm{l}\kappa_e}(\mathrm{i}\,\widetilde{\omega}_\mathrm{r}\Omega_\mathrm{l} + \mathrm{e}^{-\mathrm{i}\varphi}J\Omega_\mathrm{r})/f, \\
T_{c_\mathrm{r}c_\mathrm{l}} &= \sqrt{\kappa_\mathrm{l}\kappa_\mathrm{r}}(\mathrm{i}\,\mathrm{e}^{\mathrm{i}\varphi}J\widetilde{\omega}_e + \Omega_\mathrm{l}\Omega_\mathrm{r})/f, \\
T_{c_\mathrm{r}c_\mathrm{r}} &= \kappa_\mathrm{r}(-\widetilde{\omega}_\mathrm{l}\widetilde{\omega}_e - \Omega_\mathrm{l}^2)/f - 1,
\end{aligned} \tag{A6}$$

$$\begin{aligned}
T_{c_\mathrm{r}e} &= \sqrt{\kappa_\mathrm{r}\kappa_e}(\mathrm{e}^{\mathrm{i}\varphi}J\Omega_\mathrm{l} + \mathrm{i}\,\widetilde{\omega}_\mathrm{l}\Omega_\mathrm{r})/f, \\
T_{ec_\mathrm{l}} &= \sqrt{\kappa_\mathrm{l}\kappa_e}(\mathrm{i}\,\widetilde{\omega}_\mathrm{r}\Omega_\mathrm{l} + \mathrm{e}^{\mathrm{i}\varphi}J\Omega_\mathrm{r})/f, \\
T_{ec_\mathrm{r}} &= \sqrt{\kappa_\mathrm{r}\kappa_e}(\mathrm{e}^{-\mathrm{i}\varphi}J\Omega_\mathrm{l} + \mathrm{i}\,\widetilde{\omega}_\mathrm{l}\Omega_\mathrm{r})/f,
\end{aligned} \tag{A7}$$

$$T_{ee} = \kappa_e(-J^2 - \widetilde{\omega}_\mathrm{l}\widetilde{\omega}_\mathrm{r})/f - 1, \tag{A8}$$

where $f = J^2\widetilde{\omega}_e + \widetilde{\omega}_\mathrm{l}\widetilde{\omega}_\mathrm{r}\widetilde{\omega}_e + \widetilde{\omega}_\mathrm{r}\Omega_\mathrm{l}^2 - 2\mathrm{i}J\Omega_\mathrm{l}\Omega_\mathrm{r}\cos\varphi + \widetilde{\omega}_\mathrm{l}\Omega_\mathrm{r}^2$.

Acknowledgments

Project supported by the National Natural Science Foundation of China (Grant Nos. 12104374, 12164042, and 12264045) and the Natural Science Foundation of Gansu Province, China (Grant No. 20JR5RA526).

References

[1] Xia K Y, Nori F and Xiao M 2018 *Phys. Rev. Lett.* **121** 203602
[2] Tang L, Tang J S, Chen M Y, Nori F, Xiao M and Xia K Y 2022 *Phys. Rev. Lett.* **128** 083604
[3] Caloz C, Alù A, Tretyakov S, Sounas D, Achouri K and Deck-Léger, Zoé-Lise 2018 *Phys. Rev. Appl.* **10** 047001
[4] Wang S P, Ridolfo A, Li T F, Savasta S, Nori F, Nakamura Y and You J Q 2023 *Nat. Commun.* **14** 4397
[5] Wang Z Y, Qian J, Wang Y P, Li J and You J Q 2023 *Appl. Phys. Lett.* **123** 153904
[6] Zhang S C, Lin G W, Hu Y Q, Qi Y H, Niu Y P and Gong S Q 2020 *Phys. Rev. Appl.* **14** 024032
[7] Liu Y C, Xiao Y F, Luan X S, Gong Q H and Wong C W 2015 *Phys. Rev. A* **91** 033818
[8] Huang R, Miranowicz A, Liao J Q, Nori F and Jing H 2018 *Phys. Rev. Lett.* **121** 153601
[9] Bin Q, Jing H, Wu Y, Nori F and Lü X Y 2024 *Phys. Rev. Lett.* **133** 043601

[10] Zhang X Z, Tian L and Li Y 2018 *Phys. Rev. A* **97** 043818
[11] Jiang Y, Maayani S, Carmon T, Nori F and Jing H 2018 *Phys. Rev. Appl.* **10** 064037
[12] Ullah, Muhiba, Mikki and Saida 2024 *Adv. Quantum Technol.* **7** 2400007
[13] Bin Q, Jing H, Wu Y, Nori F and Lü X Y 2024 *Phys. Rev. Lett.* **133** 043601
[14] Tian L and Li Z 2017 *Phys. Rev. A* **96** 013808
[15] Xu X W, Chen A X, Li Y and Liu Y X 2017 *Phys. Rev. A* **96** 053853
[16] Lai D G, Huang J F, Yin X L, Hou B P, Li W L, Vitali D, Nori F and Liao J Q 2020 *Phys. Rev. A* **102** 011502(R)
[17] Rozas G, Bruchhausen A E, Fainstein A, Jusserand B and Lemaître A 2014 *Phys. Rev. B* **90** 201302
[18] Fainstein A, Lanzillotti-Kimura A D, Jusserand B and Perrin B 2013 *Phys. Rev. Lett.* **110** 037403
[19] Jusserand B, Poddubny A N, Poshakinskiy A V, Fainstein A and Lemaitre A 2015 *Phys. Rev. Lett.* **115** 267402
[20] Ballarini D, Giorgi M D, Cancellieri E, Houdré R, Giacobino E, Cingolani R, Bramati A, Gigli G and Sanvitto D 2013 *Nat. Commun.* **4** 1778
[21] Huang X and Liu Y C 2023 *Phys. Rev. A* **107** 023703
[22] Wouters M and Carusotto I 2007 *Phys. Rev. Lett.* **99** 140402
[23] Tang J, Zhang J, Lv Y C, Wang H, Xu F F, Zhang C, Sun L X, Yao J N and Zhao Y S 2021 *Nat. Commun.* **12** 3265
[24] Chen G, Bonadeo N H, Steel D G, Gammon D, Katzer D S, Park D and Sham L J 2000 *Science* **289** 1906
[25] Cancellieri E, Marchetti F M, Szymańska M H and Tejedor C 2011 *Phys. Rev. B* **83** 214507
[26] Laussy F P, Malpuech G, Kavokin A and Bigenwald P 2004 *Phys. Rev. Lett.* **93** 016402
[27] Zasedatelev A V, Baranikov A V, Urbonas D, Scafirimuto F, Scherf U, Stöferle T, Mahrt R F and Lagoudakis P G 2019 *Nat. Photon.* **13** 378
[28] Xu X W and Li Y 2015 *Phys. Rev. A* **91** 053854
[29] Xu X W and Li Y 2014 *Phys. Rev. Lett.* **112** 076402
[30] Demenev A A, Yaremkevich D D, Scherbakov A V, Kulakovskii V D, Gavrilov S S, Yakovlev D R and Bayer M 2022 *Phys. Rev. Appl.* **18** 044045
[31] Takao Aokia, Barak Dayan, Wilcut E, Bowenb W P, Parkinsc A S and Kimble H J 2006 *Nature* **443** 671
[32] Lai Y H, Lu Y K, Suh M G, Yuan Z Q and Vahala K 2019 *Nature* **576** 65
[33] Tian C, Chen L Q, Zhang Y J, Zhu L Q, Hu W P, Pan Y C, Wang Z, Zhang F X, Zhang L, Dong H X and Zhou W H 2022 *Nano Lett.* **22** 3026
[34] Zhu L Q, Pan Y C, Chen L Q, Wang Z, Zhang F X, Yang G R, Huang C C, Hu W P, Zhang L, Zhang Y J, Dong H X and Zhou W H 2023 *Nano Lett.* **23** 7797
[35] Weis S, Riviere R, Deleglise S, Gavartin E, Arcizet O, Schliesser A and Kippenberg T J 2010 *Science* **330** 1520
[36] Santos P V and Fainstein A 2023 *Opt. Mater. Express* **13** 1974
[37] Demirchyan S S, Chestnov I Y, Alodjants A P, Glazov M M and Kavokin A V 2014 *Phys. Rev. Lett.* **112** 196403